

Bridging doubly heavy tetraquark mass spectrum with heavy baryons utilizing heavy antiquark-diquark symmetry*

Liu-Yu Zhang (张刘宇)¹ Tian-Wei Wu (吴天伟)^{1†}  Yong-Liang Ma (马永亮)^{2‡} 

¹School of Science, Shenzhen Campus of Sun Yat-sen University, Shenzhen 518107, China

²School of Frontier Sciences, Nanjing University, Suzhou 215163, China

Abstract: Motivated by the observation of the doubly charmed tetraquark $T_{cc}(3875)^+$, we present a systematic study of doubly heavy tetraquarks ($T_{QQ'\bar{q}\bar{q}'}$) using heavy antiquark-diquark symmetry (HADS) within a constituent quark model. By calibrating model parameters to known hadron spectra and incorporating the effective mass formula, we predict the masses for 38 ground-state tetraquarks with cc , bb , and bc heavy quark pairs, including the non-strange, single-strange, and double-strange configurations with quantum numbers $J^P = 0^+, 1^+$ and 2^+ . Notably, we identify several stable states below the relevant meson-meson thresholds, particularly in the $bb\bar{q}\bar{q}'$ sector. The explicit connection between the doubly heavy tetraquark and the heavy baryon spectra through HADS reduces model dependence and reveals the fundamental systematics in the heavy-quark hadron landscape.

Keywords: hadron physics, tetraquark, exotic hadrons

DOI: 10.1088/1674-1137/ae3f0b **CSTR:** 32044.14.ChinesePhysicsC.50053105

I. INTRODUCTION

The discovery of exotic hadrons beyond the conventional quark-antiquark (meson) and three-quark (baryon) paradigms stands as a pivotal achievement of modern particle physics. Since 2003, many exotic hadronic states that cannot be well understood by the conventional constituent quark model have been observed. Typically, in the heavy flavor sector, the observations of the so-called X, Y, Z states, the tetraquarks, the pentaquarks and so forth, have extended the hadron spectra and deepened our understanding of the strong interactions between quarks in the nonperturbative region (see, *e.g.*, Refs. [1–11] for reviews).

In 2017, the doubly heavy baryon Ξ_{cc}^{++} was discovered in the $\Lambda_c^+ K^- \pi^+ \pi^+$ mass spectrum by the LHCb collaboration with a mass of 3621.4 MeV [12], which is the first observed doubly heavy hadron. The observation of the doubly charmed tetraquark candidate $T_{cc}^+(3875)$ by the LHCb collaboration in 2021 marked a highlight moment [13, 14]. Its striking proximity to the $D^{*+}D^0$ mass threshold (within ~ 360 keV) and narrow width ignited intense theoretical debate concerning its fundamental nature. Two primary interpretations emerged: a loosely bound hadronic molecule held together by residual strong

forces between D^* and D mesons [15–19], and a compact tetraquark state with internal structure dominated by strong, short-distance correlations within the $c\bar{c}u\bar{d}$ valence quarks [20–23]. Overall, no study has determined the internal structure and nature of $T_{cc}(3875)^+$; doubly heavy tetraquarks need further investigations to reveal their nature. While both pictures can qualitatively accommodate the mass and quantum numbers of the $T_{cc}^+(3875)$, they predict significantly different properties for its partners and the broader spectrum of doubly heavy tetraquarks (DHTs). Unambiguously resolving this structural dichotomy remains a central challenge and has aroused interests in studies on the doubly heavy hadrons both theoretically and experimentally [15–47].

Current theoretical efforts to map the DHTs landscape employ diverse methodologies. In Ref. [20], the authors have successfully predicted the existence of DHTs before the discovery of $T_{cc}(3875)^+$ employing the constituent quark model with a good light quark symmetry. The masses of tetraquarks have been calculated in the framework of the diquark-antidiquark picture in the relativistic quark model [40], in a relativized quark model within the variational method [42], and an extended chromomagnetic model [44]. Refs. [34, 41] systematically

Received 10 August 2025; Accepted 29 January 2026; Accepted manuscript online 30 January 2026

* The work of Tian-Wei Wu is supported by the National Natural Science Foundation of China (12405108). Yong-Liang Ma is supported in part by the National Science Foundation of China (NSFC) (12347103) and Gusu Talent Innovation Program (ZXL2024363)

[†] E-mail: wutw6@mail.sysu.edu.cn

[‡] E-mail: ylma@nju.edu.cn



Content from this work may be used under the terms of the Creative Commons Attribution 3.0 licence. Any further distribution of this work must maintain attribution to the author(s) and the title of the work, journal citation and DOI. Article funded by SCOAP³ and published under licence by Chinese Physical Society and the Institute of High Energy Physics of the Chinese Academy of Sciences and the Institute of Modern Physics of the Chinese Academy of Sciences and IOP Publishing Ltd

studied the mass splittings of DHT states with the color-magnetic interaction by considering color mixing effects and roughly estimate their masses. The masses and magnetic moments of tetraquarks were computed in a unified framework of the MIT bag model [43] and diffusion Monte Carlo method (DMC) [45]. In Ref. [46], the authors used DMC to calculate the DHT system in two kinds of constituent quark models: the pure constituent quark model AL1/AP1 and chiral constituent quark model.

Phenomenological quark models offer intuitive structural insights, yet conventional treatments often yield masses systematically higher than experimental candidates, suggesting the necessity of incorporating crucial dynamical correlations. A powerful organizing principle emerges from heavy-quark symmetry. In the heavy quark mass limit ($m_Q \rightarrow \infty$, $Q = c, b$), the spin of the heavy quark decouples and heavy diquark shares the same color structure as heavy antiquark, giving rise to a heavy antiquark-diquark symmetry [48–50] (HADS, also known as super flavor symmetry [51–53]). HADS establishes an approximate symmetry between the color-antitriplet heavy diquark (QQ) in a doubly heavy baryon ($QQ'q$, $q = u, d, s$) and the color-triplet heavy antiquark (\bar{Q}) in a heavy-light meson ($\bar{Q}q$). Consequently, the spectrum of doubly heavy baryons (Ξ_{cc} , Ξ_{bb} , Ω_{cc} , etc.) and heavy-light mesons ($D^{(*)}$, $B^{(*)}$, $D_s^{(*)}$, etc.) exhibit remarkable parallels dictated by light degrees of freedom [53–55]. Crucially, this symmetry extends to compact DHTs ($QQ'\bar{q}\bar{q}'$), where the QQ' diquark core plays a role analogous to the single heavy antiquark \bar{Q} , whereas the light antidiquark ($\bar{q}\bar{q}'$) remains unchanged. The $QQ'\bar{q}\bar{q}'$ tetraquark spectrum should therefore reflect symmetries connecting the $\bar{Q}\bar{q}\bar{q}'$ baryon spectrum.

In this work, we leverage the profound implications of HADS within a robust constituent quark model (CQM) framework to systematically investigate the mass spectrum of DHT states. Our approach transcends the limitations of treating tetraquarks in isolation by explicitly incorporating the symmetry connecting compact tetraquarks to the well-established spectra of heavy baryons and mesons. This imposes stringent constraints on model dynamics and predicted masses. We employ a sophisticated CQM incorporating effective mass formula calibrated on established hadron spectra [23, 56–58]. Within this framework, we construct compact tetraquark configurations where the QQ' pair forms a colored antitriplet diquark, and the light $\bar{q}\bar{q}'$ pair forms a color triplet, combining to color-singlet states. Our study delivers comprehensive predictions for the ground states of $cc\bar{q}\bar{q}'$, $bb\bar{q}\bar{q}'$, and $bc\bar{q}\bar{q}'$ systems with various light quark flavors and quantum numbers. We critically compare predictions for T_{cc} and its partners with experimental data and other theoretical approaches. Key spectral features—state ordering, hyperfine splittings, and proximity to meson-meson thresholds—serve as discriminants between compact tetra-

quark and molecular interpretations. Furthermore, we predict masses and quantum numbers for unobserved states, providing essential guidance for experimental searches at LHCb, Belle II, and PANDA.

The rest of this paper is structured as follows: Sec. II introduces the doubly heavy tetraquark configurations within HADS, the constituent quark model, and the mass formulas. Sec. III presents the predicted mass spectra with the corresponding meson-meson thresholds and a comparison with other studies. Sec. IV summarizes the study.

II. THEORETICAL FRAMEWORK

In this section, we will first introduce the HADS that correlates the DHTs with heavy baryons. Subsequently, we will elaborate on how to utilize HADS to construct the configurations of DHT states that are correlated with heavy baryons. Finally, we will explain how to calculate the mass spectra of these doubly heavy tetraquarks using the mass formulas derived from the constituent quark model.

HADS is a significant concept in the study of hadronic physics [48–50, 59]. In the limit of heavy quark masses approaching infinity in Quantum Chromodynamics (QCD), this symmetry emerges, connecting the properties of hadrons with two heavy quarks QQ' to those with one heavy antiquark \bar{Q} . Physically, HADS arises when a diquark pair forms a tightly bound, nearly point-like object. For instance, the attraction between two heavy quarks in a diquark comes from a color Coulombic interaction in the color 3_c channel. When the quark masses are large enough, the heavy quarks move slowly, acting like non-relativistic particle sources in a Coulombic potential. As the size of a Coulombic bound state is inversely proportional to its mass (for a fixed coupling), in the large mass limit, the diquark becomes a heavy, small object with color $\bar{3}_c$, effectively acting as a static point-like $\bar{3}_c$ color source, similar to a heavy antiquark.

This symmetry has important implications for understanding the spectra and properties of hadrons. It relates the quark structure of doubly heavy baryons to that of heavy antimesons. For example, the masses of $\Xi_{cc}^{(*)}$ baryons and $D^{(*)}$ mesons serve the relation $m_{\Xi_{cc}^{(*)}} - m_{\Xi_{cc}} = 3/4(m_{\bar{D}^*} - m_{\bar{D}})$, which has been numerically confirmed with the masses observed by experiments ($m_{\Xi_{cc}^{(*)}}$, $m_{\bar{D}^*}$ and $m_{\bar{D}}$) and lattice QCD simulations ($m_{\Xi_{cc}^{(*)}}$) [60–63]. Along this line, the masses and configurations of DHTs can also be related to those of heavy baryons by leveraging HADS, which relates DHTs to heavy baryons by treating the double-heavy diquark (QQ') as a heavy antiquark \bar{X} . Combined with the constituent quark model—well-established for describing meson and baryon spectra—this symmetry allows us to predict the mass spectrum of DHTs systematically. We extend previous studies to include not only doubly charmed (T_{cc}) and doubly bot-

tomed (T_{bb}) states but also bottom-charmed (T_{bc}) configurations, covering non-strange, single-strange, and double-strange light quark combinations. The predicted states span spin-parity quantum numbers 0^+ , 1^+ , and 2^+ , providing a complete landscape of the ground states of DHTs.

A. Configurations of DHTs

The configurations of DHTs are labeled with $[[\bar{q}\bar{q}]_s^c[QQ]_S^C]_J^I$, where C and S denote the color and spin of the heavy diquark QQ , respectively. c and s denote the color and spin of the light diquark $\bar{q}\bar{q}$, respectively. I is the isospin of the tetraquark, and J is the total angular momentum of the tetraquark. DHTs with different number of strange quarks have different configurations. Since we are establishing a connection between DHTs and heavy baryons, we assign c and C to be 3 and $\bar{3}$, respectively. Color sextet combinations may also exist in the color structure of DHT states. However, such configurations have not been experimentally observed to date. In diquarks, the Casimir coefficient for the $3_c \otimes 3_c = 6_c$ representation is $1/3$, indicating a repulsive interaction between the two quarks in this color configuration, whereas the coefficient for $3_c \otimes 3_c = \bar{3}_c$ is $-2/3$, suggesting a strong attractive interaction. Therefore, $3_c \otimes 3_c = \bar{3}_c$ is likely the dominant form of diquark coupling. Ref. [42] shows that the weight of the latter configuration in DHT states exceeds 90%. Based on these theoretical and experimental reasons, in this work, we consider only the 3_c and $\bar{3}_c$ color configurations for diquarks. The values of s and S can be either 0 or 1, depending on the flavor combination of the tetraquark. The configurations are listed below with three combinations in the order of the number of strange quarks; unflavored light quarks are denoted as n with $n = u, d$.

1. DHTs with non-strange light quarks

(a) Configuration $[[\bar{n}\bar{n}]_s^3[QQ]_1^3]_J^I$:

$$\begin{aligned} & [[\bar{n}\bar{n}]_0^3[QQ]_1^3]_1^0 \\ & [[\bar{n}\bar{n}]_1^3[QQ]_1^3]_1^1 \\ & [[\bar{n}\bar{n}]_1^3[QQ]_1^3]_1^1 \\ & [[\bar{n}\bar{n}]_1^3[QQ]_1^3]_1^2 \end{aligned}$$

(b) Configuration $[[\bar{n}\bar{n}]_s^3[cb]_S^{\bar{3}}]_J^I$:

$$\begin{aligned} & [[\bar{n}\bar{n}]_0^3[cb]_0^{\bar{3}}]_0^0 \\ & [[\bar{n}\bar{n}]_0^3[cb]_1^{\bar{3}}]_1^0 \\ & [[\bar{n}\bar{n}]_1^3[cb]_0^{\bar{3}}]_1^1 \\ & [[\bar{n}\bar{n}]_1^3[cb]_1^{\bar{3}}]_1^1 \\ & [[\bar{n}\bar{n}]_1^3[cb]_1^{\bar{3}}]_1^1 \\ & [[\bar{n}\bar{n}]_1^3[cb]_1^{\bar{3}}]_1^2 \end{aligned}$$

2. DHTs with single-strange light quarks

(a) Configuration $[[\bar{n}\bar{s}]_s^3[QQ]_1^3]_J^I$:

$$\begin{aligned} & [[\bar{n}\bar{s}]_0^3[QQ]_1^3]_1^{\frac{1}{2}} \\ & [[\bar{n}\bar{s}]_1^3[QQ]_1^3]_0^{\frac{1}{2}} \\ & [[\bar{n}\bar{s}]_1^3[QQ]_1^3]_1^{\frac{1}{2}} \\ & [[\bar{n}\bar{s}]_1^3[QQ]_1^3]_2^{\frac{1}{2}} \end{aligned}$$

(b) Configuration $[[\bar{n}\bar{s}]_s^3[cb]_S^{\bar{3}}]_J^I$:

$$\begin{aligned} & [[\bar{n}\bar{s}]_0^3[cb]_0^{\bar{3}}]_0^{\frac{1}{2}} \\ & [[\bar{n}\bar{s}]_0^3[cb]_1^{\bar{3}}]_1^{\frac{1}{2}} \\ & [[\bar{n}\bar{s}]_1^3[cb]_0^{\bar{3}}]_1^{\frac{1}{2}} \\ & [[\bar{n}\bar{s}]_1^3[cb]_1^{\bar{3}}]_0^{\frac{1}{2}} \\ & [[\bar{n}\bar{s}]_1^3[cb]_1^{\bar{3}}]_1^{\frac{1}{2}} \\ & [[\bar{n}\bar{s}]_1^3[cb]_1^{\bar{3}}]_2^{\frac{1}{2}} \end{aligned}$$

3. DHTs with double-strange quarks:

(a) Configuration $[[\bar{s}\bar{s}]_1^3[QQ]_1^3]_J^I$:

$$\begin{aligned} & [[\bar{s}\bar{s}]_1^3[QQ]_1^3]_0 \\ & [[\bar{s}\bar{s}]_1^3[QQ]_1^3]_1 \\ & [[\bar{s}\bar{s}]_1^3[QQ]_1^3]_2 \end{aligned}$$

(b) Configuration $[[\bar{s}\bar{s}]_1^3[cb]_S^{\bar{3}}]_J^I$:

$$\begin{aligned} & [[\bar{s}\bar{s}]_1^3[cb]_0^{\bar{3}}]_1 \\ & [[\bar{s}\bar{s}]_1^3[cb]_1^{\bar{3}}]_0 \\ & [[\bar{s}\bar{s}]_1^3[cb]_1^{\bar{3}}]_1 \\ & [[\bar{s}\bar{s}]_1^3[cb]_1^{\bar{3}}]_2 \end{aligned}$$

B. Mass formula of DHT in CQM

In this subsection, we use a well established mass formula in CQM that has been successful in interpreting the spectra of mesons and baryons [23, 56, 58], to calculate the masses of DHTs with HADS. In Ref. [20], this model was used to study the doubly heavy tetraquarks with a good light quark symmetry and successfully predict the mass of $T_{cc}(3875)$. In Ref. [23], the ground states of heavy baryon spectrum is well described with the mass formula

$$M_B = \sum_i m_i + \sum_{i<j} (F_i \cdot F_j) [B_{ij} + (\sigma_i \cdot \sigma_j) \alpha_{ij} / m_i m_j], \quad (1)$$

where m_i, B_{ij} and α_{ij} are the mass of the i th constituent quark and the binding and hyperfine spin coupling constant between the i th and j th quarks, respectively. F_i, σ_i are the color and spin operators with $i, j = 1, 2, 3$. This simple formula yields a standard mass variance of $\chi_M = 7.6$ MeV. The method has been successfully extended to doubly charmed and doubly bottomed tetraquarks with non-strange light quarks [23]. We extend the previous investigations to the bottom-charmed sector and cases with non-, single-, and double-strange quark(s). Thus, the complete mass spectrum of the whole ground states of DHTs correlated to the heavy baryons is displayed.

The mass formula in CQM can be extended to DHT with HADS as

$$M_{\text{DHT}} = m_{[QQ']_S^c qq'} + \sum_{i<j} (F_i \cdot F_j) [B_{ij} + (\sigma_i \cdot \sigma_j) \alpha_{ij} / m_i m_j], \quad (2)$$

where $m_{[QQ']_S^c qq'} = m_{[QQ']_S^c} + m_q + m_{q'}$ is the constituent mass of the quark components, with $m_{[QQ']_S^c}$ and $m_{q^{(\prime)}}$ representing the effective masses of heavy diquark and light quark, respectively. The coefficients of color structure operators are determined by the color representations of the quark components and the group theory of $SU(3)_c$, which is $-2/3$ for $\bar{3}_c$ representation between two quarks in baryons. B_{ij} and α_{ij} are the bindings and spin hyperfine coupling constants between the light quarks and those between the diquark $[QQ']_S^c$ and the light quark. The effective mass of the heavy diquark $m_{[QQ']_S^c}$ can also be determined by the mass formula in CQM:

$$m_{[QQ']_S^c} = m_Q + m_{Q'} + F_Q \cdot F_{Q'} \left[B_{QQ'} + \frac{\alpha_{QQ'} \sigma_Q \cdot \sigma_{Q'}}{m_Q m_{Q'}} \right], \quad (3)$$

where $m_{Q^{(\prime)}}$ is the heavy quark mass. The quark masses, bindings, and spin hyperfine coupling constants are needed to calculate the mass of the heavy diquark $[QQ']_S^c$.

The required parameters are listed in Table 1, and their values are determined by fitting the baryon spectra and corresponding hidden-flavor and bottom-charmed heavy mesons [20, 58]. It should be noted that the masses

of constituent quarks in baryons are different from those in mesons. In this work, since quarks are in the form of diquarks, all the quark masses adopted for calculating the mass spectra are based on the quark masses within baryons. Only when determining the hyperfine splitting constants $\alpha_{QQ'}$ and binding energies $B_{QQ'}$ between heavy quarks, given that the corresponding heavy baryons have not yet been experimentally observed, we resort to meson masses for such determinations. Taking bb as an example, since $m_{\Upsilon_b} = 2m_b^m + (-4/3)[B_{bb}^m + \alpha_{bb}/(m_b^m)^2]$ and $m_{\eta_b} = 2m_b^m + (-4/3)[B_{bb}^m - 3\alpha_{bb}/(m_b^m)^2]$, we have $\alpha_{bb}/(m_b^m)^2 \approx \alpha_{bb}/(m_b^m)^2 = -3/16(m_{\Upsilon_b} - m_{\eta_b}) = -11.6$ MeV and $B_{bb} \approx B_{bb}^m = -3/16[(3m_{\Upsilon_b} + m_{\eta_b}) - 8m_b^m] = 422.0$ MeV, neglecting the small differences in the constituent quark masses between baryons and mesons. The meson masses are taken from experiments and the heavy quark mass in mesons $m_b^m = 5003.8$ MeV and $m_c^m = 1663.2$ MeV (the superscript m/b denotes in mesons/baryons) are from Ref. [58] within the same model. For B_{cb} and α_{cb} , since B_c^* has not been observed yet, we refer to the theoretical predictions. In this work, we use the value in Ref. [58], $m_{B_c^*} - m_{B_c} = 68$ MeV, which is determined by an interpolation method with the mass differences $m_{\Upsilon_b} - m_{\eta_b} = 62.3$ MeV and $m_{J/\psi} - m_{\eta_c} = 113.2$ MeV. The four heavy meson masses are from experiments, and the interpolation method is based on the same constituent quark model as in this work. Other theoretical predictions of $m_{B_c^*} - m_{B_c}$ are also alternative; for example, the lattice prediction yields a value of 55(3) MeV [64]. The former value yields $B_{bc} = 256.2$ MeV and $\alpha_{cb}/(m_b m_c) = 12.7$ MeV, whereas the latter value yields $B_{bc} = 263.5$ MeV and $\alpha_{cb}/(m_b m_c) = 10.3$ MeV. This results in a shift of less than 10 MeV in the finally obtained T_{bc} mass spectrum, which does not affect the main results and conclusions of this paper. We adopt the former value $m_{B_c^*} - m_{B_c} = 68$ MeV considering model consistency and the fact that according to the heavy quark spin symmetry, the spin mass splitting of bc mesons $m_{B_c^*} - m_{B_c}$ should lie between that of cc and bb mesons.

The masses of the heavy diquarks are determined to be $m_{[cc]_1^3} = 2m_c^b + (-2/3)(B_{cc} + \alpha_{cc}/(m_c^b)^2) = 3300.8$ MeV, $m_{[bb]_1^3} = 2m_b^b + (-2/3)(B_{bb} + \alpha_{bb}/(m_b^b)^2) = 9821.0$ MeV, $m_{[cb]_0^3} = m_c^b + m_b^b + (-2/3)(B_{cb} - 3\alpha_{cb}/(m_b^b \cdot m_c^b)) = 6567.0$ MeV, and $m_{[cb]_1^3} = m_c^b + m_b^b + (-2/3)(B_{cb} + \alpha_{cb}/(m_b^b \cdot m_c^b)) = 6600.9$ MeV. After determining the mass of the heavy diquark $m_{[QQ']_S^c}$, we need the binding and spin hyperfine coupling con-

Table 1. Masses, bindings, and spin hyperfine splittings of baryons in CQM (in unit of MeV).

Parameters	m_n	m_s	m_c	m_b	B_{cs}	B_{bs}
Values	364.3	536.2	1715.9	5047.3	53.4	62.6
B_{cc}	B_{cb}	B_{bb}	α/m_n^2	α_{cc}/m_c^2	$\alpha_{cb}/m_c m_b$	α_{bb}/m_b^2
217.7	256.2	422.0	-76.8	-21.2	-12.7	-11.6

stant between $[QQ']_S^c$ and the light quark to calculate the masses of DHTs using Eq. (2). Refs. [20, 56, 58] indicate that there are no bindings between the light quark pair (qq') and heavy-unflavored quark pair Qn . Since the color and spin operators have been explicitly introduced in Eq. (2), the binding between heavy diquark and light quark should be independent of both color and spin, denoted as $B_{[QQ']_q}$. Therefore, we have $B_{[QQ']_q} = B_{Qq} + B_{Q'q}$, resulting in $B_{[QQ']_n} = 0$, $B_{[cc]_s} = 2B_{cs} = 106.8$ MeV, $B_{[bb]_s} = 2B_{bs} = 125.2$ MeV, and $B_{[cb]_s} = B_{cs} + B_{bs} = 116.0$ MeV. For the spin hyperfine coupling constant α_{ij} , the constant is the same for the light-light quarks and heavy-light quarks but is flavor dependent for the heavy-heavy quarks. For $\alpha_{[QQ']_S^c q}$, since the heavy diquark is regarded as a heavy quark X with HADS, $\alpha_{[QQ']_S^c q}$ should be α_{Xq} , which is proved to be independent of the mass of heavy quark X and share the same value as $\alpha_{qq'}$ (abbreviated as α). For detailed discussions, refer to Refs. [20, 56, 58].

It should be noted that the hyperfine splitting constant α_{ij} is model-dependent [23, 41, 65], whereas the hyperfine splitting $\alpha_{ij}/m_i m_j$, combined with the spin factor, reflects the mass splitting of different spin configurations of DHTs. According to HADS, the spin splitting should approach zero in the heavy quark limit. This is reflected in Table I: spin splitting decreases as the heavy quark mass increases ($|\alpha_{cc}/m_c^2| > |\alpha_{cb}/m_c m_b| > |\alpha_{bb}/m_b^2|$). The impact of HADS symmetry breaking is also worth discussing. In this work, HADS only affects the hyperfine splitting between the heavy diquark and light quark. We therefore define $\chi_{\text{HADS}} = |\mathcal{A}_{\text{HADS}}(F_{[QQ']_S^c} \cdot F_q)(\sigma_{[QQ']_S^c} \cdot \sigma_q) \alpha_{[QQ']_S^c q}/m_q m_{[QQ']_S^c}|$, where $\mathcal{A}_{\text{HADS}}$ is defined as the degree of HADS breaking. Considering 25% breaking of HADS [23, 54], the uncertainties of HADS χ_{HADS} in this work are estimated to be at the level of 11.3 MeV, 5.7 MeV, and 3.8 MeV for the doubly charmed, bottom-charmed, and doubly bottomed tetraquarks, respectively.

The masses, bindings, and spin hyperfine splittings needed for calculating the masses of DHTs are listed in Table 2. It should be noted that no new parameters are introduced here. All parameters used to calculate the masses of DHTs are derived from the 13 independent parameters already listed in Table 1, which are obtained by fitting the experimental data of the observed hadron mass spectra. This approach ensures correlation between the theoretical predictions of DHT masses and the experimental data of baryon mass spectra, thereby enhancing the reliability of the predictions in this work.

III. RESULTS AND DISCUSSIONS

In this section, we use the mass formula introduced in the last section with the parameters listed in Table 2 to calculate the mass spectra of DHTs. Based on different combinations of quark flavors and quantum numbers, we predict and calculate the masses of 38 DHT states linked to heavy baryons through HADS. This includes:

- 14 DHT partners of Λ_Q and Σ_Q baryons:
 - 6 partners for isospin-0 Λ_Q baryons
 - 8 partners for isospin-1 Σ_Q baryons
- 14 DHT partners of Ξ_Q baryons
- 10 DHT partners of Ω_Q baryons

The masses, quantum numbers, configurations, and mass formulas of the 38 predicted DHTs are systematically categorized and presented across Tables 3, 4, and 5. It should be noted that the states listed in the tables are calculated one-to-one according to configurations using the mass formula. Actually, since certain configurations share the same quantum numbers and quark components, mixing can occur between them. We can compute the correlation matrix of states with different configurations to determine the eigenmasses and eigenvectors of the mixed eigenstates, thereby obtaining the mass spectrum of DHT states considering mixing effects. The diagonal elements of the correlation matrix correspond to the masses of explicit configurations given in Tables 3, 4, and 5, whereas the off-diagonal elements represent the couplings between different configurations under the mass Hamiltonian (*i.e.*, Eq.(2)). This coupling originates from the different projections of color operators and spin operators onto different configurations. Considering that we adopt HADS in this work, treating the heavy diquark as an integral anti-heavy quark, configurations $[QQ']_1^3$ and $[QQ']_0^3$ are regarded as distinct "particles" and cannot mix. Consequently, the mixing of DHT states is simplified to a form similar to the mixing of three-quark heavy baryon configurations. This is a key distinction between the present work and other studies. By comparing the mass spectrum of mixed states with and without the HADS approximation, we can assess the impact of introducing HADS on the DHT mass spectrum.

In Table 6, we present the mass correlation matrices

Table 2. Masses, bindings, and hyperfine couplings of quarks in doubly heavy tetraquark ground states (in unit of MeV).

Parameters	$m_{[cc]_1^3}$	$m_{[bb]_1^3}$	$m_{[cb]_0^3}$	$m_{[cb]_1^3}$
Values	3300.8	9821.0	6567.0	6600.9
Parameters	$B_{[cc]_s}$	$B_{[bb]_s}$	$B_{[cb]_s}$	$\alpha/m_q m_{[cc]_1^3}$
Values	106.8	125.2	116.0	-8.5

Table 3. Doubly heavy tetraquark ground states aroused from heavy anti-baryons $\bar{\Lambda}_c$ ($\bar{\Lambda}_b$) and $\bar{\Sigma}_c$ ($\bar{\Sigma}_b$) with HADS.

State	Configuration	$I(J^P)$	Mass formula
$T_{cc}(3876)$	$[[\bar{n}\bar{n}]_0^3[cc]_1^3]_1^0$	$0(1^+)$	$2m_n^b + m_{[cc]_1^3} + 2\alpha/(m_n^b)^2$
$T_{cc}(4035)$	$[[\bar{n}\bar{n}]_1^3[cc]_1^3]_1^1$	$1(0^+)$	$2m_n^b + m_{[cc]_1^3} - \frac{2}{3}[\alpha/(m_n^b)^2 - 8\alpha_{[cc]_1^3 n}/(m_n^b m_{[cc]_1^3})]$
$T_{cc}(4058)$	$[[\bar{n}\bar{n}]_1^3[cc]_1^3]_1^1$	$1(1^+)$	$2m_n^b + m_{[cc]_1^3} - \frac{2}{3}[\alpha/(m_n^b)^2 - 4\alpha_{[cc]_1^3 n}/(m_n^b m_{[cc]_1^3})]$
$T_{cc}(4103)$	$[[\bar{n}\bar{n}]_1^3[cc]_1^3]_1^2$	$1(2^+)$	$2m_n^b + m_{[cc]_1^3} - \frac{2}{3}[\alpha/(m_n^b)^2 + 4\alpha_{[cc]_1^3 n}/(m_n^b m_{[cc]_1^3})]$
$T_{bb}(10396)$	$[[\bar{n}\bar{n}]_0^3[bb]_1^3]_1^0$	$0(1^+)$	$2m_n^b + m_{[bb]_1^3} + 2\alpha/(m_n^b)^2$
$T_{bb}(10586)$	$[[\bar{n}\bar{n}]_1^3[bb]_1^3]_1^0$	$1(0^+)$	$2m_n^b + m_{[bb]_1^3} - \frac{2}{3}[\alpha/(m_n^b)^2 - 8\alpha_{[bb]_1^3 n}/(m_n^b m_{[bb]_1^3})]$
$T_{bb}(10593)$	$[[\bar{n}\bar{n}]_1^3[bb]_1^3]_1^1$	$1(1^+)$	$2m_n^b + m_{[bb]_1^3} - \frac{2}{3}[\alpha/(m_n^b)^2 - 4\alpha_{[bb]_1^3 n}/(m_n^b m_{[bb]_1^3})]$
$T_{bb}(10608)$	$[[\bar{n}\bar{n}]_1^3[bb]_1^3]_1^2$	$1(2^+)$	$2m_n^b + m_{[bb]_1^3} - \frac{2}{3}[\alpha/(m_n^b)^2 + 4\alpha_{[bb]_1^3 n}/(m_n^b m_{[bb]_1^3})]$
$T_{cb}(7142)$	$[[\bar{n}\bar{n}]_0^3[cb]_1^3]_1^0$	$0(0^+)$	$2m_n^b + m_{[cb]_1^3} + 2\alpha/(m_n^b)^2$
$T_{cb}(7176)$	$[[\bar{n}\bar{n}]_0^3[cb]_1^3]_1^0$	$0(1^+)$	$2m_n^b + m_{[cb]_1^3} + 2\alpha/(m_n^b)^2$
$T_{cb}(7347)$	$[[\bar{n}\bar{n}]_1^3[cb]_1^3]_1^1$	$1(1^+)$	$2m_n^b + m_{[cb]_1^3} - (2/3)[\alpha/(m_n^b)^2]$
$T_{cb}(7358)$	$[[\bar{n}\bar{n}]_1^3[cb]_1^3]_1^1$	$1(0^+)$	$2m_n^b + m_{[cb]_1^3} - (2/3)[\alpha/(m_n^b)^2 - 8\alpha/(m_n^b m_{[cb]_1^3})]$
$T_{cb}(7369)$	$[[\bar{n}\bar{n}]_1^3[cb]_1^3]_1^1$	$1(1^+)$	$2m_n^b + m_{[cb]_1^3} - (2/3)[\alpha/(m_n^b)^2 - 4\alpha/(m_n^b m_{[cb]_1^3})]$
$T_{cb}(7392)$	$[[\bar{n}\bar{n}]_1^3[cb]_1^3]_1^2$	$1(2^+)$	$2m_n^b + m_{[cb]_1^3} - (2/3)[\alpha/(m_n^b)^2 + 4\alpha/(m_n^b m_{[cb]_1^3})]$

Table 4. Doubly heavy tetraquark ground states aroused from heavy anti-baryons $\bar{\Omega}_c$ ($\bar{\Omega}_b$) with HADS.

State	Configuration	J^P	Mass formula
$T_{cc\bar{s}\bar{s}}(4224)$	$[[\bar{s}\bar{s}]_1^3[cc]_1^3]_0$	0^+	$2m_s^b + m_{[cc]_1^3} - (2/3)[2B_{[cc]_1^3 s} + \alpha/(m_s^b)^2 - 8\alpha/(m_s^b m_{[cc]_1^3})]$
$T_{cc\bar{s}\bar{s}}(4239)$	$[[\bar{s}\bar{s}]_1^3[cc]_1^3]_1$	1^+	$2m_s^b + m_{[cc]_1^3} - (2/3)[2B_{[cc]_1^3 s} + \alpha/(m_s^b)^2 - 4\alpha/(m_s^b m_{[cc]_1^3})]$
$T_{cc\bar{s}\bar{s}}(4270)$	$[[\bar{s}\bar{s}]_1^3[cc]_1^3]_2$	2^+	$2m_s^b + m_{[cc]_1^3} - (2/3)[2B_{[cc]_1^3 s} + \alpha/(m_s^b)^2 + 4\alpha/(m_s^b m_{[cc]_1^3})]$
$T_{bb\bar{s}\bar{s}}(10740)$	$[[\bar{s}\bar{s}]_1^3[bb]_1^3]_0$	0^+	$2m_s^b + m_{[bb]_1^3} - (2/3)[2B_{[bb]_1^3 s} + \alpha/(m_s^b)^2 - 8\alpha/(m_s^b m_{[bb]_1^3})]$
$T_{bb\bar{s}\bar{s}}(10745)$	$[[\bar{s}\bar{s}]_1^3[bb]_1^3]_1$	1^+	$2m_s^b + m_{[bb]_1^3} - (2/3)[2B_{[bb]_1^3 s} + \alpha/(m_s^b)^2 - 4\alpha/(m_s^b m_{[bb]_1^3})]$
$T_{bb\bar{s}\bar{s}}(10755)$	$[[\bar{s}\bar{s}]_1^3[bb]_1^3]_2$	2^+	$2m_s^b + m_{[bb]_1^3} - (2/3)[2B_{[bb]_1^3 s} + \alpha/(m_s^b)^2 + 4\alpha/(m_s^b m_{[bb]_1^3})]$
$T_{cb\bar{s}\bar{s}}(7508)$	$[[\bar{s}\bar{s}]_1^3[cb]_1^3]_1$	1^+	$2m_s^b + m_{[cb]_1^3} - (2/3)[2B_{[cb]_1^3 s} + \alpha/(m_s^b)^2]$
$T_{cb\bar{s}\bar{s}}(7527)$	$[[\bar{s}\bar{s}]_1^3[cb]_1^3]_0$	0^+	$2m_s^b + m_{[cb]_1^3} - (2/3)[2B_{[cb]_1^3 s} + \alpha/(m_s^b)^2 - 8\alpha/(m_s^b m_{[cb]_1^3})]$
$T_{cb\bar{s}\bar{s}}(7535)$	$[[\bar{s}\bar{s}]_1^3[cb]_1^3]_1$	1^+	$2m_s^b + m_{[cb]_1^3} - (2/3)[2B_{[cb]_1^3 s} + \alpha/(m_s^b)^2 - 4\alpha/(m_s^b m_{[cb]_1^3})]$
$T_{cb\bar{s}\bar{s}}(7550)$	$[[\bar{s}\bar{s}]_1^3[cb]_1^3]_2$	2^+	$2m_s^b + m_{[cb]_1^3} - (2/3)[2B_{[cb]_1^3 s} + \alpha/(m_s^b)^2 + 4\alpha/(m_s^b m_{[cb]_1^3})]$

of different configurations under the same quantum numbers considering HADS, along with the final eigenmasses and eigenvectors. The results indicate that mixing primarily occurs for the quantum number $1/2(1^+)$: T_{cc} , T_{bb} , and T_{bc} each have two configurations that undergo mixing, with mass differences of approximately several MeV to over ten MeV compared to the unmixed cases. In the alternative scenario where we do not consider the HADS approximation and still treat DHT as a four-body system, the projection values of color operators and spin operators can be found in Tables II and III of Ref. [46]. The results for this case are listed in Table 7. Compared to the HADS-included case, T_{cb} has seven additional mixed configurations, mainly due to the allowable mix-

ing between $[cb]_1^3$ and $[cb]_0^3$ without HADS. A comparison of the results in Tables 6 and 7 shows that the introduction of HADS has an impact of approximately ten-odd MeV on the masses of mixed DHT states, consistent with the aforementioned analysis.

The masses and quantum numbers of the 38 predicted DHTs with mixing effect are categorized and presented across Tables 8, 9, and 10. These encompass three distinct groups: 14 states linked to $\bar{\Lambda}_c/\bar{\Lambda}_b$ and $\bar{\Sigma}_c/\bar{\Sigma}_b$ baryons, 14 states associated with $\bar{\Xi}_c/\bar{\Xi}_b$ baryons, and 10 states corresponding to $\bar{\Omega}_c/\bar{\Omega}_b$ baryons. Each table provides comparative mass predictions from multiple theoretical approaches, revealing an overall consistency in spectral hierarchies, particularly the mass ordering

Table 5. Doubly heavy tetraquark ground states aroused from heavy anti-baryons $\bar{\Xi}_c$ ($\bar{\Xi}_b$) with HADS.

State	Configuration	$I(J^P)$	Mass formula
$T_{cc\bar{s}}$ (4026)	$[[\bar{n}\bar{s}]_0^3[cc]_1^{\bar{3}}]_1^{\frac{1}{2}}$	$\frac{1}{2}(1^+)$	$m_n^b + m_s^b + m_{[cc]_1^{\bar{3}}} - (2/3)[B_{[cc]_1^{\bar{3}}s} - 3\alpha/(m_n^b m_s^b)]$
$T_{cc\bar{s}}$ (4127)	$[[\bar{n}\bar{s}]_1^3[cc]_1^{\bar{3}}]_0^{\frac{1}{2}}$	$\frac{1}{2}(0^+)$	$m_n^b + m_s^b + m_{[cc]_1^{\bar{3}}} - (2/3)[B_{[cc]_1^{\bar{3}}s} + \alpha/(m_n^b m_s^b) - 4\alpha/(m_n^b m_{[cc]_1^{\bar{3}}}) - 4\alpha/(m_s^b m_{[cc]_1^{\bar{3}}})]$
$T_{cc\bar{s}}$ (4146)	$[[\bar{n}\bar{s}]_1^3[cc]_1^{\bar{3}}]_1^{\frac{1}{2}}$	$\frac{1}{2}(1^+)$	$m_n^b + m_s^b + m_{[cc]_1^{\bar{3}}} - (2/3)[B_{[cc]_1^{\bar{3}}s} + \alpha/(m_n^b m_s^b) - 2\alpha/(m_n^b m_{[cc]_1^{\bar{3}}}) - 2\alpha/(m_s^b m_{[cc]_1^{\bar{3}}})]$
$T_{cc\bar{s}}$ (4184)	$[[\bar{n}\bar{s}]_1^3[cc]_1^{\bar{3}}]_{1/2}^{\frac{1}{2}}$	$\frac{1}{2}(2^+)$	$m_n^b + m_s^b + m_{[cc]_1^{\bar{3}}} - (2/3)[B_{[cc]_1^{\bar{3}}s} + \alpha/(m_n^b m_s^b) + 2\alpha/(m_n^b m_{[cc]_1^{\bar{3}}}) + 2\alpha/(m_s^b m_{[cc]_1^{\bar{3}}})]$
$T_{bb\bar{s}}$ (10534)	$[[\bar{n}\bar{s}]_0^3[bb]_1^{\bar{3}}]_1^{\frac{1}{2}}$	$\frac{1}{2}(1^+)$	$m_n^b + m_s^b + m_{[bb]_1^{\bar{3}}} - (2/3)[B_{[bb]_1^{\bar{3}}s} - 3\alpha/(m_n^b m_s^b)]$
$T_{bb\bar{s}}$ (10660)	$[[\bar{n}\bar{s}]_1^3[bb]_1^{\bar{3}}]_0^{\frac{1}{2}}$	$\frac{1}{2}(0^+)$	$m_n^b + m_s^b + m_{[bb]_1^{\bar{3}}} - (2/3)[B_{[bb]_1^{\bar{3}}s} + \alpha/(m_n^b m_s^b) - 4\alpha/(m_n^b m_{[bb]_1^{\bar{3}}}) - 4\alpha/(m_s^b m_{[bb]_1^{\bar{3}}})]$
$T_{bb\bar{s}}$ (10666)	$[[\bar{n}\bar{s}]_1^3[bb]_1^{\bar{3}}]_1^{\frac{1}{2}}$	$\frac{1}{2}(1^+)$	$m_n^b + m_s^b + m_{[bb]_1^{\bar{3}}} - (2/3)[B_{[bb]_1^{\bar{3}}s} + \alpha/(m_n^b m_s^b) - 2\alpha/(m_n^b m_{[bb]_1^{\bar{3}}}) - 2\alpha/(m_s^b m_{[bb]_1^{\bar{3}}})]$
$T_{bb\bar{s}}$ (10679)	$[[\bar{n}\bar{s}]_1^3[bb]_1^{\bar{3}}]_{1/2}^{\frac{1}{2}}$	$\frac{1}{2}(2^+)$	$m_n^b + m_s^b + m_{[bb]_1^{\bar{3}}} - (2/3)[B_{[bb]_1^{\bar{3}}s} + \alpha/(m_n^b m_s^b) + 2\alpha/(m_n^b m_{[bb]_1^{\bar{3}}}) + 2\alpha/(m_s^b m_{[bb]_1^{\bar{3}}})]$
$T_{cb\bar{s}}$ (7286)	$[[\bar{n}\bar{s}]_0^3[cb]_0^{\bar{3}}]_0^{\frac{1}{2}}$	$\frac{1}{2}(0^+)$	$m_n^b + m_s^b + m_{[cb]_0^{\bar{3}}} - (2/3)[B_{[cb]_0^{\bar{3}}s} - 3\alpha/(m_n^b m_s^b)]$
$T_{cb\bar{s}}$ (7320)	$[[\bar{n}\bar{s}]_0^3[cb]_1^{\bar{3}}]_1^{\frac{1}{2}}$	$\frac{1}{2}(1^+)$	$m_n^b + m_s^b + m_{[cb]_1^{\bar{3}}} - (2/3)[B_{[cb]_1^{\bar{3}}s} - 3\alpha/(m_n^b m_s^b)]$
$T_{cb\bar{s}}$ (7425)	$[[\bar{n}\bar{s}]_1^3[cb]_0^{\bar{3}}]_1^{\frac{1}{2}}$	$\frac{1}{2}(1^+)$	$m_n^b + m_s^b + m_{[cb]_0^{\bar{3}}} - (2/3)[B_{[cb]_0^{\bar{3}}s} + \alpha/(m_n^b m_s^b)]$
$T_{cb\bar{s}}$ (7440)	$[[\bar{n}\bar{s}]_1^3[cb]_1^{\bar{3}}]_0^{\frac{1}{2}}$	$\frac{1}{2}(0^+)$	$m_n^b + m_s^b + m_{[cb]_1^{\bar{3}}} - (2/3)[B_{[cb]_1^{\bar{3}}s} + \alpha/(m_n^b m_s^b) - 4\alpha/(m_n^b m_{[cb]_1^{\bar{3}}}) - 4\alpha/(m_s^b m_{[cb]_1^{\bar{3}}})]$
$T_{cb\bar{s}}$ (7449)	$[[\bar{n}\bar{s}]_1^3[cb]_1^{\bar{3}}]_1^{\frac{1}{2}}$	$\frac{1}{2}(1^+)$	$m_n^b + m_s^b + m_{[cb]_1^{\bar{3}}} - (2/3)[B_{[cb]_1^{\bar{3}}s} + \alpha/(m_n^b m_s^b) - 2\alpha/(m_n^b m_{[cb]_1^{\bar{3}}}) - 2\alpha/(m_s^b m_{[cb]_1^{\bar{3}}})]$
$T_{cb\bar{s}}$ (7468)	$[[\bar{n}\bar{s}]_1^3[cb]_1^{\bar{3}}]_{1/2}^{\frac{1}{2}}$	$\frac{1}{2}(2^+)$	$m_n^b + m_s^b + m_{[cb]_1^{\bar{3}}} - (2/3)[B_{[cb]_1^{\bar{3}}s} + \alpha/(m_n^b m_s^b) + 2\alpha/(m_n^b m_{[cb]_1^{\bar{3}}}) + 2\alpha/(m_s^b m_{[cb]_1^{\bar{3}}})]$

Table 6. Eigenmasses and eigenvectors of the DHT states with quantum numbers and mixing configurations with HADS.

$I(J^P)$	Configuration	$\langle H \rangle / \text{MeV}$	Mass/MeV	Eigenvector
$\frac{1}{2}(1^+)$	$[[\bar{n}\bar{s}]_0^3[cc]_1^{\bar{3}}]_1^{\frac{1}{2}}$	$\begin{pmatrix} 4026 & 40 \\ 40 & 4146 \end{pmatrix}$	[4014]	$\begin{bmatrix} (-0.957, 0.290) \\ (0.290, 0.957) \end{bmatrix}$
	$[[\bar{n}\bar{s}]_1^3[cc]_1^{\bar{3}}]_1^{\frac{1}{2}}$		[4158]	
$\frac{1}{2}(1^+)$	$[[\bar{n}\bar{s}]_0^3[bb]_1^{\bar{3}}]_1^{\frac{1}{2}}$	$\begin{pmatrix} 10534 & 13 \\ 13 & 10666 \end{pmatrix}$	[10533]	$\begin{bmatrix} (-0.995, 0.097) \\ (0.097, 0.995) \end{bmatrix}$
	$[[\bar{n}\bar{s}]_1^3[bb]_1^{\bar{3}}]_1^{\frac{1}{2}}$		[10667]	
$\frac{1}{2}(1^+)$	$[[\bar{n}\bar{s}]_0^3[cb]_1^{\bar{3}}]_1^{\frac{1}{2}}$	$\begin{pmatrix} 7320 & 20 \\ 20 & 7449 \end{pmatrix}$	[7317]	$\begin{bmatrix} (-0.989, 0.150) \\ (0.150, 0.989) \end{bmatrix}$
	$[[\bar{n}\bar{s}]_1^3[cb]_1^{\bar{3}}]_1^{\frac{1}{2}}$		[7452]	

$T_{QQ} < T_{QQ\bar{s}} < T_{QQ\bar{s}\bar{s}}$, while highlighting method-dependent variations in absolute values. Notably, our predictions derive from a framework exploiting HADS to establish rigorous connections between tetraquark spectra and the experimentally measured heavy baryon spectrum. This approach contrasts with complementary methodologies: relativistic quark models employing diquark-antidiquark configurations [40] or variational methods [42]; effective interaction models including color-magnetic interactions [41] and extended chromomagnetic model [44]; and non-perturbative techniques such as diffusion Monte Carlo [45] and MIT bag model calculations [43].

The tabulated comparisons demonstrate that our HADS-constrained predictions show closer agreement with near-threshold states like T_{cc} (3876) while providing systematic coverage of strange quark effects across all

configurations. Unlike molecular models that struggle with hyperfine splittings, our approach delivers precise mass differences between spin partners, a critical discriminator for exotic state identification. These comprehensive spectral predictions establish reliable benchmarks for experimental searches at LHCb and Belle II while underscoring HADS as a fundamental symmetry bridging conventional baryon and exotic tetraquark spectroscopy.

The mass spectra of DHTs are presented in Figs. 1, 2 and 3, which reveal systematic patterns across different flavor sectors. All figures share common features: states are categorized by J^P quantum numbers (0^+ , 1^+ , 2^+) and color-coded by strangeness content (non-strange: red, single-strange: blue, double-strange: black), with dashed lines indicating relevant meson-meson thresholds.

Figure 1 displays the doubly charmed tetraquark

Table 7. Eigenmasses and eigenvectors of the DHT states with quantum numbers and mixing configurations without HADS.

$I(J^P)$	Configuration	$\langle H \rangle / \text{MeV}$	Mass/MeV	Eigenvector
$\frac{1}{2}(1^+)$	$[[\bar{n}\bar{s}]_0^3[cc]_1^{\frac{3}{2}}]_1^{\frac{1}{2}}$	$\begin{pmatrix} 4026 & -10 \\ -10 & 4128 \end{pmatrix}$	[4025]	$\begin{bmatrix} (0.995, 0.097) \\ (-0.097, 0.995) \end{bmatrix}$
	$[[\bar{n}\bar{s}]_1^3[cc]_1^{\frac{3}{2}}]_1^{\frac{1}{2}}$		[4129]	
$\frac{1}{2}(1^+)$	$[[\bar{n}\bar{s}]_0^3[bb]_1^{\frac{3}{2}}]_1^{\frac{1}{2}}$	$\begin{pmatrix} 10534 & -3 \\ -3 & 10660 \end{pmatrix}$	[10534]	$\begin{bmatrix} (0.999, 0.023) \\ (-0.023, 0.999) \end{bmatrix}$
	$[[\bar{n}\bar{s}]_1^3[bb]_1^{\frac{3}{2}}]_1^{\frac{1}{2}}$		[10660]	
$1(1^+)$	$[[\bar{n}\bar{n}]_1^3[cb]_0^{\frac{3}{2}}]_1^1$	$\begin{pmatrix} 7347 & 20 \\ 20 & 7351 \end{pmatrix}$	[7329]	$\begin{bmatrix} (-0.741, 0.671) \\ (0.671, 0.741) \end{bmatrix}$
	$[[\bar{n}\bar{n}]_1^3[cb]_1^{\frac{3}{2}}]_1^1$		[7369]	
$\frac{1}{2}(0^+)$	$[[\bar{n}\bar{s}]_0^3[cb]_0^{\frac{3}{2}}]_0^{\frac{1}{2}}$	$\begin{pmatrix} 7286 & -4 \\ -4 & 7410 \end{pmatrix}$	[7286]	$\begin{bmatrix} (0.999, 0.032) & (-0.032, 0.999) \end{bmatrix}$
	$[[\bar{n}\bar{s}]_1^3[cb]_1^{\frac{3}{2}}]_0^{\frac{1}{2}}$		[7410]	
$\frac{1}{2}(1^+)$	$[[\bar{n}\bar{s}]_0^3[cb]_1^{\frac{3}{2}}]_1^{\frac{1}{2}}$	$\begin{pmatrix} 7320 & 2 & -7 \\ 2 & 7425 & 17 \\ -7 & 17 & 7434 \end{pmatrix}$	[7319]	$\begin{bmatrix} (0.997, -0.029, 0.065) \\ (-0.063, -0.796, 0.603) \\ (-0.034, 0.605, 0.795) \end{bmatrix}$
	$[[\bar{n}\bar{s}]_1^3[cb]_0^{\frac{3}{2}}]_1^{\frac{1}{2}}$		[7412]	
	$[[\bar{n}\bar{s}]_1^3[cb]_1^{\frac{3}{2}}]_1^{\frac{1}{2}}$		[7447]	
(1^+)	$[[\bar{s}\bar{s}]_1^3[cb]_0^{\frac{3}{2}}]_1$	$\begin{pmatrix} 7508 & 14 \\ 14 & 7522 \end{pmatrix}$	[7499]	$\begin{bmatrix} (-0.851, 0.526) \\ (0.526, 0.851) \end{bmatrix}$
	$[[\bar{s}\bar{s}]_1^3[cb]_1^{\frac{3}{2}}]_1$		[7531]	

Table 8. Spectrum of DHTs aroused from heavy anti-baryons $\bar{\Lambda}_c(\bar{\Lambda}_b)$ and $\bar{\Sigma}_c(\bar{\Sigma}_b)$ with HADS (values in brackets are without HADS) in this work and comparisons with different models or methods. DMC: diffusion Monte Carlo method. CMI: color-magnetic interaction model; RQM(VM): relativized quark model within the variational method; RQM(DA): relativized quark model within diquark-antidiquark picture; MIT: MIT bag model; ECM: extended chromomagnetic model.

$I(J^P)$	Configuration	This work	DMC [45]	CMI [41]	MIT [43]	RQM(VM) [42]	RQM(DA) [40]	ECM I [44]	ECM II [44]
$0(1^+)$	$[[\bar{n}\bar{n}]_0^3[cc]_1^{\frac{3}{2}}]_1^0$	3876	3892	4007	3925	4041	3935	3749.8	3868.7
$1(0^+)$	$[[\bar{n}\bar{n}]_1^3[cc]_1^{\frac{3}{2}}]_0^1$	4035	4062	4078	4032	4159	4056	3833.2	3969.2
$1(1^+)$	$[[\bar{n}\bar{n}]_1^3[cc]_1^{\frac{3}{2}}]_1^1$	4058	4104	4021	4117	4268	4079	3946.4	4053.2
$1(2^+)$	$[[\bar{n}\bar{n}]_1^3[cc]_1^{\frac{3}{2}}]_2^1$	4103	4207	4271	4179	4318	4118	4017.1	4123.8
$0(1^+)$	$[[\bar{n}\bar{n}]_0^3[bb]_1^{\frac{3}{2}}]_1^0$	10396	10,338	10686	10654	10550	10502	10291.6	10390.9
$1(0^+)$	$[[\bar{n}\bar{n}]_1^3[bb]_1^{\frac{3}{2}}]_0^1$	10586	10,624	10841	10834	10765	10648	10468.8	10569.3
$1(1^+)$	$[[\bar{n}\bar{n}]_1^3[bb]_1^{\frac{3}{2}}]_1^1$	10593	10,680	10875	10854	10779	10657	10485.3	10584.2
$1(2^+)$	$[[\bar{n}\bar{n}]_1^3[bb]_1^{\frac{3}{2}}]_2^1$	10608	10702	10897	10878	10799	10673	10507.9	10606.8
$0(0^+)$	$[[\bar{n}\bar{n}]_0^3[cb]_0^{\frac{3}{2}}]_0^0$	7142	7108	7256	7260	7297	7239	7003.4	7124.6
$0(1^+)$	$[[\bar{n}\bar{n}]_0^3[cb]_1^{\frac{3}{2}}]_1^0$	7176	7084	7321	7288	7325	7246	7046.2	7158.0
$1(0^+)$	$[[\bar{n}\bar{n}]_1^3[cb]_1^{\frac{3}{2}}]_0^1$	735	7396	7457	7438	7519	7383	7189.5	7305.6
$1(1^+)$	$[[\bar{n}\bar{n}]_1^3[cb]_0^{\frac{3}{2}}]_1^1$	7347(7329)	7510	7473	7465	7537	7396	7211.0	7322.5
	$[[\bar{n}\bar{n}]_1^3[cb]_1^{\frac{3}{2}}]_1^1$	7369(7369)	7542	7548	7509	7561	7403	7211.0	7322.5
$1(2^+)$	$[[\bar{n}\bar{n}]_1^3[cb]_1^{\frac{3}{2}}]_2^1$	7392	7568	7582	7531	7586	7422	7293.2	7396.0

($T_{cc\bar{q}\bar{q}'}$) spectrum, with a total of 11 particles, consisting of 3 $T_{cc\bar{s}\bar{s}}$ states, 4 $T_{cc\bar{s}}$ states, and 5 T_{cc} states. Notably, the $T_{cc}(3876)$ state with $J^P = 1^+$ aligns closely with the experimentally observed $T_{cc}^+(3875)$, positioned near the $D^{*+}D^0$ threshold. The $T_{ccs}(4014)$ mass is above the DD_s^* and D^*D_s thresholds but below that of $D^*D_s^*$, while the other $T_{cc\bar{q}\bar{q}'}$ states lie above the relevant meson-pair thresholds. Figure 2 shows the mass spectrum of ground

doubly bottomed heavy tetraquarks $T_{bb\bar{q}\bar{q}'}$. The numbers of $T_{bb\bar{q}\bar{q}'}$ in Fig. 2 are consistent with that in Fig. 1 because they share the same configurations. However, unlike the ground doubly charmed heavy tetraquarks, many states exist with masses below the corresponding meson pair thresholds. All the states in the 1^+ and 2^+ configurations are below the corresponding meson pair masses, particularly the $T_{bb}(10396)$ with $J^P = 1^+$, which sits ~ 160

Table 9. Spectrum of DHTs aroused from heavy anti-baryons $\bar{\Xi}_c$ ($\bar{\Xi}_b$) with HADS (values in brackets are without HADS) in this work and comparisons with different models or methods. DMC: diffusion Monte Carlo method. CMI: color-magnetic interaction model; RQM(VM): relativized quark model within the variational method; RQM(DA): relativized quark model within diquark-antidiquark picture; MIT: MIT bag model; ECM: extended chromomagnetic model.

$I(J^P)$	Configuration	This work	DMC [45]	CMI [41]	MIT [43]	RQM(VM) [42]	RQM(DA) [40]	ECM I [44]	ECM II [44]
$\frac{1}{2}(0^+)$	$[[\bar{n}\bar{s}]_1^3[cc]_1^{\bar{3}}]_0^{\frac{1}{2}}$	4127	4165	4236	4165	4323	4221	3937.6	4085.7
$\frac{1}{2}(1^+)$	$[[\bar{n}\bar{s}]_0^3[cc]_1^{\bar{3}}]_1^{\frac{1}{2}}$	4014(4025)	4056	4225	4091	4232	4143	3919.0	4051.5
	$[[\bar{n}\bar{s}]_1^3[cc]_1^{\bar{3}}]_1^{\frac{1}{2}}$	4158(4129)	4128	4363	4247	4394	4239	4073.0	4180.2
$\frac{1}{2}(2^+)$	$[[\bar{n}\bar{s}]_1^3[cc]_1^{\bar{3}}]_2^{\frac{1}{2}}$	4184	4314	4434	4305	4440	4271	4144.3	4251.5
$\frac{1}{2}(0^+)$	$[[\bar{n}\bar{s}]_1^3[bb]_1^{\bar{3}}]_0^{\frac{1}{2}}$	10660	10721	10999	10955	10883	10802	10586.4	10684.1
$\frac{1}{2}(1^+)$	$[[\bar{n}\bar{s}]_0^3[bb]_1^{\bar{3}}]_1^{\frac{1}{2}}$	10533(10534)	10684	10911	10811	10734	10706	10473.1	10569.0
	$[[\bar{n}\bar{s}]_1^3[bb]_1^{\bar{3}}]_1^{\frac{1}{2}}$	10667(10660)	10736	11010	10974	10897	10809	10605.3	10700.5
$\frac{1}{2}(2^+)$	$[[\bar{n}\bar{s}]_1^3[bb]_1^{\bar{3}}]_2^{\frac{1}{2}}$	10679	10747	11060	10997	10915	10823	10628.7	10723.9
$\frac{1}{2}(0^+)$	$[[\bar{n}\bar{s}]_0^3[cb]_0^{\bar{3}}]_0^{\frac{1}{2}}$	7286(7286)	–	7461	–	7483	7444	7156.5	7296.2
	$[[\bar{n}\bar{s}]_1^3[cb]_1^{\bar{3}}]_0^{\frac{1}{2}}$	7440(7410)	–	7615	–	7643	7540	7299.0	7421.0
$\frac{1}{2}(1^+)$	$[[\bar{n}\bar{s}]_0^3[cb]_1^{\bar{3}}]_1^{\frac{1}{2}}$	7317(7319)	–	7530	–	7514	7451	7212.8	7336.1
	$[[\bar{n}\bar{s}]_1^3[cb]_1^{\bar{3}}]_1^{\frac{1}{2}}$	7452(7447)	–	7706	–	7682	7552	7330.5	7487.8
	$[[\bar{n}\bar{s}]_1^3[cb]_0^{\bar{3}}]_1^{\frac{1}{2}}$	7425(7412)	–	7634	–	7659	7555	7323.9	7440.9
$\frac{1}{2}(2^+)$	$[[\bar{n}\bar{s}]_1^3[cb]_1^{\bar{3}}]_2^{\frac{1}{2}}$	7468	–	7718	–	7705	7572	7415.1	7517.1

Table 10. Spectrum of DHTs aroused from heavy anti-baryons $\bar{\Omega}_c$ ($\bar{\Omega}_b$) with HADS (values in brackets are without HADS) in this work and comparisons with different models or methods. DMC: diffusion Monte Carlo method. CMI: color-magnetic interaction model; RQM(VM): relativized quark model within the variational method; RQM(DA): relativized quark model within diquark-antidiquark picture; MIT: MIT bag model; ECM: extended chromomagnetic model.

J^P	Configuration	This work	DMC [45]	CMI [41]	MIT [43]	RQM(VM) [42]	RQM(DA) [40]	ECM I [44]	ECM II [44]
0^+	$[[\bar{s}\bar{s}]_1^3[cc]_1^{\bar{3}}]_0$	4224	4205	4395	4300	4417	4359	4043.7	4199.1
1^+	$[[\bar{s}\bar{s}]_1^3[cc]_1^{\bar{3}}]_1$	4239	4323	4526	4382	4493	4375	4192.6	4300.2
2^+	$[[\bar{s}\bar{s}]_1^3[cc]_1^{\bar{3}}]_2$	4270	4381	4597	4433	4536	4402	4264.5	4372.1
0^+	$[[\bar{s}\bar{s}]_1^3[bb]_1^{\bar{3}}]_0$	10740	10868	11157	11078	10972	10932	10697.1	10792.1
1^+	$[[\bar{s}\bar{s}]_1^3[bb]_1^{\bar{3}}]_1$	10745	10908	11199	11099	10986	10939	10718.2	10809.8
2^+	$[[\bar{s}\bar{s}]_1^3[bb]_1^{\bar{3}}]_2$	10755	10926	11224	11119	11004	10950	10742.5	10834.1
0^+	$[[\bar{s}\bar{s}]_1^3[cb]_1^{\bar{3}}]_0$	7527	7653	7774	7693	7735	7673	7404.4	7531.3
1^+	$[[\bar{s}\bar{s}]_1^3[cb]_0^{\bar{3}}]_1$	7508(7499)	7711	7793	7716	7752	7683	7431.8	7553.6
	$[[\bar{s}\bar{s}]_1^3[cb]_1^{\bar{3}}]_1$	7535(7531)	7764	7872	7757	7775	7684	7503.3	7603.5
2^+	$[[\bar{s}\bar{s}]_1^3[cb]_1^{\bar{3}}]_2$	7550	7862	7908	7779	7798	7701	7534.3	7633.8

MeV beneath the B^*B threshold, suggesting exceptional stability. By contrast, in the 0^+ configuration, the $T_{bb\bar{s}\bar{s}}$ (10740) is slightly higher than $\bar{B}_s\bar{B}_s$ threshold, $T_{bb\bar{s}}$ (10660) is higher than $\bar{B}\bar{B}_s$, and T_{bb} (10586) is higher than $\bar{B}\bar{B}$, respectively. Figure 3 shows the bottom-charm $T_{bc\bar{q}\bar{q}'}$ sector, featuring 13 states due to asymmetric spin couplings. Among them, there are 4 $T_{cb\bar{s}\bar{s}}$ states, 6 $T_{cb\bar{s}}$ states, and 6 T_{cb} states. Among the five states in 0^+ con-

figuration, $T_{cb\bar{s}}$ (7286) is higher than $D\bar{B}_s$ and $D_s\bar{B}$, but much lower than $D_s^*\bar{B}^*$ and $D^*\bar{B}_s^*$, T_{cb} (7142) is below the $D\bar{B}$ threshold, while the remaining states are above the corresponding meson pair thresholds. In the 1^+ and 2^+ configurations, most of the $T_{bc\bar{q}\bar{q}'}$ states are above the corresponding meson-meson thresholds, except $T_{cb\bar{s}}$ (7317), which is above the threshold of $D\bar{B}_s^*$ but below that of $D^*\bar{B}_s$.

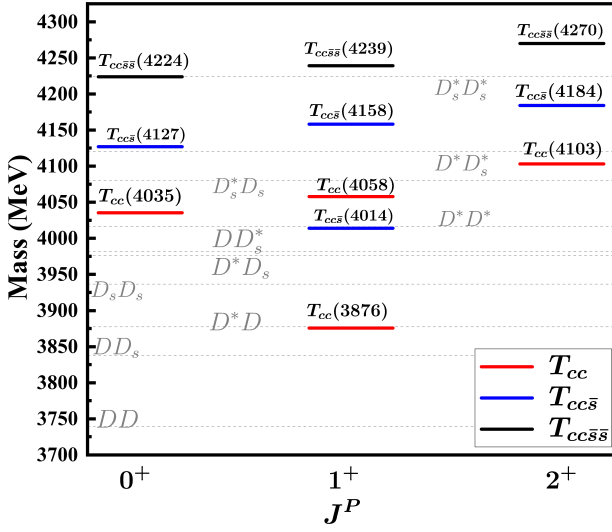


Fig. 1. (color online) Mass spectrum and spin-parity of doubly charmed tetraquarks with nonstrange (red), single-strange (blue) and double-strange quarks (black).

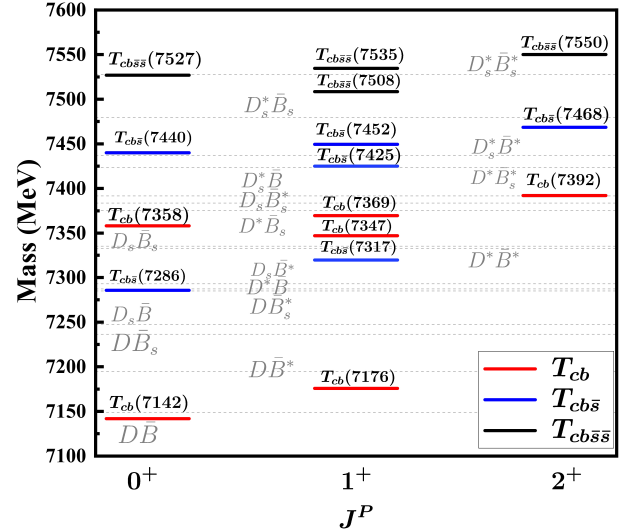


Fig. 3. (color online) Mass spectrum and spin-parity of bottom-charmed tetraquarks with nonstrange (red), single-strange (blue) and double-strange quarks (black).

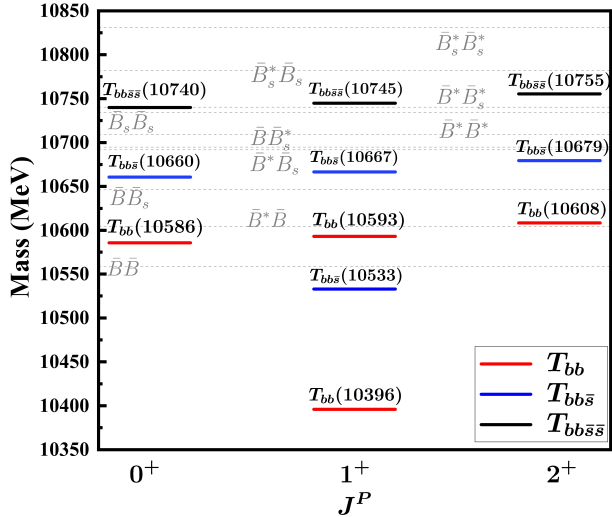


Fig. 2. (color online) Mass spectrum and spin-parity of doubly bottomed tetraquarks with nonstrange (red), single-strange (blue) and double-strange quarks (black).

Common characteristics include the universal mass hierarchy $T_{QQ'} < T_{QQ'\bar{s}} < T_{QQ'\bar{s}\bar{s}}$, reduced hyperfine splittings in heavier flavor sectors, and enhanced binding for b -quark systems due to diminished kinetic energy. The progressive stabilization from cc to bb systems highlights the mass-dependence of binding mechanisms. Furthermore, by systematically comparing the obtained mass spectrum of DHTs with the corresponding meson-meson thresholds, we find that most of the DHT masses are above or far from the thresholds. Considering that molecular states are generally close to and below the thresholds, this provides crucial diagnostics for distinguishing compact tetraquarks from corresponding mo-

lecular states.

IV. SUMMARY

In this work, we provide a comprehensive investigation of the DHTs ($T_{QQ\bar{q}\bar{q}'}$) spectrum using HADS within a well-accepted constituent quark model framework calibrated to established hadron data. By correlating $QQ\bar{q}\bar{q}'$ states with experimentally measured heavy baryon (QQq') spectrum through HADS, we systematically predict masses for 38 ground-state tetraquarks with $J^P = 0^+, 1^+, 2^+$ across cc , bb , and bc flavor sectors with varying strange quark content. All parameters are derived from baryon spectra fits, ensuring model consistency with QCD phenomenology without new inputs. Key findings reveal that bb -containing tetraquarks predominantly lie below the meson-meson thresholds, indicating strong binding and potential stability, whereas cc and bc configurations generally reside near or above thresholds except for specific cases like the $T_{cc}(3876)$ state that matches the observed $T_{cc}^+(3875)$. The universal mass ordering $T_{QQ'} < T_{QQ'\bar{s}} < T_{QQ'\bar{s}\bar{s}}$ and method-independent hyperfine splittings provide critical discriminants between compact tetraquarks and molecular interpretations.

Our study shows that the hyperfine splitting of DHT states decreases with an increase in the mass of heavy diquarks, which is consistent with the requirements of heavy quark symmetry. We have also estimated the impact of HADS symmetry breaking on the mass of DHTs, and found that for double-charmed, bottom-charmed, and double-bottomed tetraquark states, the impact levels are about 11.3 MeV, 5.7 MeV, and 3.8 MeV respectively. This order relationship also reflects the heavy quark mass dependence of heavy quark symmetry. These predictions

establish essential benchmarks for experimental searches at LHCb, Belle II, and PANDA, while demonstrating

HADS as a fundamental symmetry unifying conventional and exotic heavy-quark hadrons.

References

- [1] A. Hosaka, T. Iijima, K. Miyabayashi *et al.*, *PTEP* **2016**, 062C01 (2016), arXiv: 1603.09229[hep-ph]
- [2] A. Ali, J. S. Lange, and S. Stone, *Prog. Part. Nucl. Phys.* **97**, 123 (2017), arXiv: 1706.00610[hep-ph]
- [3] F. K. Guo, C. Hanhart, U. G. Meißner *et al.*, *Rev. Mod. Phys.* **90**, 015004 (2018), arXiv: 1705.00141[hep-ph]
- [4] A. Esposito, A. Pilloni, and A. D. Polosa, *Phys. Rept.* **668**, 1 (2017), arXiv: 1611.07920[hep-ph]
- [5] R. F. Lebed, R. E. Mitchell, and E. S. Swanson, *Prog. Part. Nucl. Phys.* **93**, 143 (2017), arXiv: 1610.04528[hep-ph]
- [6] J. M. Richard, *Few Body Syst.* **57**, 1185 (2016), arXiv: 1606.08593[hep-ph]
- [7] H. X. Chen, W. Chen, X. Liu *et al.*, *Phys. Rept.* **639**, 1 (2016), arXiv: 1601.02092[hep-ph]
- [8] Y. R. Liu, H. X. Chen, W. Chen *et al.*, *Prog. Part. Nucl. Phys.* **107**, 237 (2019), arXiv: 1903.11976[hep-ph]
- [9] N. Brambilla, S. Eidelman, C. Hanhart *et al.*, *Phys. Rept.* **873**, 1 (2020), arXiv: 1907.07583[hep-ex]
- [10] M. Z. Liu, Y. W. Pan, Z. W. Liu *et al.*, *Phys. Rept.* **1108**, 1 (2025), arXiv: 2404.06399[hep-ph]
- [11] Z. G. Wang, (2025), arXiv: 2502.11351[hep-ph]
- [12] R. Aaij *et al.* (LHCb Collaboration), *Phys. Rev. Lett.* **119**, 112001 (2017), arXiv: 1707.01621[hep-ex]
- [13] R. Aaij *et al.* (LHCb Collaboration), *Nature Phys.* **18**, 751 (2022), arXiv: 2109.01038[hep-ex]
- [14] R. Aaij *et al.* (LHCb Collaboration), (2021), arXiv: 2109.01056[hep-ex]
- [15] M. L. Du, V. Baru, X. K. Dong *et al.*, *Phys. Rev. D* **105**, 014024 (2022), arXiv: 2110.13765[hep-ph]
- [16] M. Padmanath and S. Prelovsek, *Phys. Rev. Lett.* **129**, 032002 (2022), arXiv: 2202.10110[hep-lat]
- [17] A. Feijoo, W. H. Liang, and E. Oset, *Phys. Rev. D* **104**, 114015 (2021), arXiv: 2108.02730[hep-ph]
- [18] L. Meng, G. J. Wang, B. Wang *et al.*, *Phys. Rev. D* **104**, 051502 (2021), arXiv: 2107.14784[hep-ph]
- [19] C. Deng and S. L. Zhu, *Phys. Rev. D* **105**, 054015 (2022), arXiv: 2112.12472[hep-ph]
- [20] M. Karliner and J. L. Rosner, *Phys. Rev. Lett.* **119**, 202001 (2017), arXiv: 1707.07666[hep-ph]
- [21] S. S. Agaev, K. Azizi, and H. Sundu, *Nucl. Phys. B* **975**, 115650 (2022), arXiv: 2108.00188[hep-ph]
- [22] Y. Kim, M. Oka, and K. Suzuki, *Phys. Rev. D* **105**, 074021 (2022), arXiv: 2202.06520[hep-ph]
- [23] T. W. Wu and Y. L. Ma, *Phys. Rev. D* **107**, L071501 (2023), arXiv: 2211.15094[hep-ph]
- [24] E. J. Eichten and C. Quigg, *Phys. Rev. Lett.* **119**, 202002 (2017), arXiv: 1707.09575[hep-ph]
- [25] Z. G. Wang and Z. H. Yan, *Eur. Phys. J. C* **78**, 19 (2018), arXiv: 1710.02810[hep-ph]
- [26] Z. G. Wang, *Acta Phys. Polon. B* **49**, 1781 (2018), arXiv: 1708.04545[hep-ph]
- [27] J. B. Cheng, S. Y. Li, Y. R. Liu *et al.*, *Chin. Phys. C* **45**, 043102 (2021), arXiv: 2008.00737[hep-ph]
- [28] R. Chen, Q. Huang, X. Liu *et al.*, *Phys. Rev. D* **104**, 114042 (2021), arXiv: 2108.01911[hep-ph]
- [29] H. Ren, F. Wu, and R. Zhu, *Adv. High Energy Phys.* **2022**, 9103031 (2022), arXiv: 2109.02531[hep-ph]
- [30] Q. Xin and Z. G. Wang, *Eur. Phys. J. A* **58**, 110 (2022), arXiv: 2108.12597[hep-ph]
- [31] M. Albaladejo, *Phys. Lett. B* **829**, 137052 (2022), arXiv: 2110.02944[hep-ph]
- [32] X. Z. Ling, M. Z. Liu, L. S. Geng *et al.*, *Phys. Lett. B* **826**, 136897 (2022), arXiv: 2108.00947[hep-ph]
- [33] S. Fleming, R. Hodges, and T. Mehen, *Phys. Rev. D* **104**, 116010 (2021), arXiv: 2109.02188[hep-ph]
- [34] T. Guo, J. Li, J. Zhao *et al.*, *Phys. Rev. D* **105**, 014021 (2022), arXiv: 2108.10462[hep-ph]
- [35] Y. Huang, H. Q. Zhu, L. S. Geng *et al.*, *Phys. Rev. D* **104**, 116008 (2021), arXiv: 2108.13028[hep-ph]
- [36] T. W. Wu, Y. W. Pan, M. Z. Liu *et al.*, *Phys. Rev. D* **105**, L031505 (2022), arXiv: 2108.00923[hep-ph]
- [37] S. Q. Luo, T. W. Wu, M. Z. Liu *et al.*, *Phys. Rev. D* **105**, 074033 (2022), arXiv: 2111.15079[hep-ph]
- [38] L. M. Abreu, *Nucl. Phys. B* **985**, 115994 (2022), arXiv: 2206.01166[hep-ph]
- [39] M. J. Yan and M. P. Valderrama, *Phys. Rev. D* **105**, 014007 (2022), arXiv: 2108.04785[hep-ph]
- [40] D. Ebert, R. N. Faustov, V. O. Galkin *et al.*, *Phys. Rev. D* **76**, 114015 (2007), arXiv: 0706.3853[hep-ph]
- [41] S. Q. Luo, K. Chen, X. Liu *et al.*, *Eur. Phys. J. C* **77**, 709 (2017), arXiv: 1707.01180[hep-ph]
- [42] Q. F. Lü, D. Y. Chen, and Y. B. Dong, *Phys. Rev. D* **102**, 034012 (2020), arXiv: 2006.08087[hep-ph]
- [43] W. X. Zhang, H. Xu, and D. Jia, *Phys. Rev. D* **104**, 114011 (2021), arXiv: 2109.07040[hep-ph]
- [44] X. Z. Weng, W. Z. Deng, and S. L. Zhu, *Chin. Phys. C* **46**, 013102 (2022), arXiv: 2108.07242[hep-ph]
- [45] H. Mutuk, *Eur. Phys. J. C* **84**, 395 (2024), arXiv: 2312.13383[hep-ph]
- [46] Y. Ma, L. Meng, Y. K. Chen *et al.*, *Phys. Rev. D* **109**, 074001 (2024), arXiv: 2309.17068[hep-ph]
- [47] L. Liu, Y. Xiao, and T. Guo, (2025), arXiv: 2505.22177[hep-ph]
- [48] M. J. Savage and M. B. Wise, *Phys. Lett. B* **248**, 177 (1990)
- [49] H. Georgi and M. B. Wise, *Phys. Lett. B* **243**, 279 (1990)
- [50] C. D. Carone, *Phys. Lett. B* **253**, 408 (1991)
- [51] Y. L. Ma and M. Harada, *Phys. Lett. B* **748**, 463 (2015), arXiv: 1503.05373[hep-ph]
- [52] Y. L. Ma and M. Harada, *Phys. Lett. B* **754**, 125 (2016), arXiv: 1510.07481[hep-ph]
- [53] Y. L. Ma and M. Harada, *J. Phys. G* **45**, 075006 (2018), arXiv: 1709.09746[hep-ph]
- [54] J. Hu and T. Mehen, *Phys. Rev. D* **73**, 054003 (2006), arXiv: hep-ph/0511321
- [55] N. Brambilla, A. Vairo, and T. Rosch, *Phys. Rev. D* **72**, 034021 (2005), arXiv: hep-ph/0506065
- [56] M. Karliner, B. Keren-Zur, H. J. Lipkin *et al.*, *Annals Phys.* **324**, 2 (2009), arXiv: 0804.1575[hep-ph]
- [57] M. Karliner, J. L. Rosner, and T. Skwarnicki, *Ann. Rev. Nucl. Part. Sci.* **68**, 17 (2018), arXiv: 1711.10626[hep-ph]

- [58] M. Karliner and J. L. Rosner, *Phys. Rev. D* **90**, 094007 (2014), arXiv: 1408.5877[hep-ph]
- [59] T. W. Wu, M. Z. Liu, L. S. Geng *et al.*, *Eur. Phys. J. C* **80**, 901 (2020), arXiv: 2004.09779[hep-ph]
- [60] M. Padmanath, R. G. Edwards, N. Mathur *et al.*, *Phys. Rev. D* **91**, 094502 (2015), arXiv: 1502.01845[hep-lat]
- [61] Y. C. Chen and T. W. Chiu (TWQCD Collaboration), *Phys. Lett. B* **767**, 193 (2017), arXiv: 1701.02581[hep-lat]
- [62] C. Alexandrou and C. Kallidonis, *Phys. Rev. D* **96**, 034511 (2017), arXiv: 1704.02647[hep-lat]
- [63] N. Mathur and M. Padmanath, *Phys. Rev. D* **99**, 031501 (2019), arXiv: 1807.00174[hep-lat]
- [64] N. Mathur, M. Padmanath, and S. Mondal, *Phys. Rev. Lett.* **121**, 202002 (2018), arXiv: 1806.04151[hep-lat]
- [65] K. K. Zhang, W. X. Zhang, and D. J. Jia, (2025), arXiv: 2503.14987[hep-ph]